DUCTILITY OF COUPLED REINFORCED MASONRY SHEAR WALLS

M. Siyam[1], W.W. El-Dakhakhni[2] and R. Drysdale[3]
[1] PhD Candidate, Department of Civil Engineering, McMaster Univ., Hamilton, Canada. siyamm@mcmaster.ca
[2] Associate Professor, Martini, Mascarin and George Chair in Masonry Design, Co-Director, Centre for Effective Design of Structures, Department of Civil Engineering, Hamilton, ON, L8S 4L7, Canada. eldak@mcmaster.ca
[3] Professor Emeritus, McMaster Univ., Hamilton, Canada. drysdale@mcmaster.ca

ABSTRACT
Coupled walls in buildings may exist around door window openings, in staicases, elevator shafts, or as a building core system. In the case of reinforced masonry (RM), the walls are connected either by concrete slabs or masonry beams. As a seismic force resisting system (SFRS), coupled walls behave somewhere between a larger wall (with an equivalent length of the two walls and their connection) and a frame system. The current Canadian reinforced conrete (RC) design provisions in the CSA A23.3, sets two separate R_d factors for ductile coupled shear walls and partially coupled shear walls. The ductile coupled shear walls are set to a value of 4.0 while the other wall type is set to 3.5. On the contrary, the current Canadian masonry code, CSA S304.1, includes no R_d factors for coupled masonry walls. Compared to RC, there has not been a as much research on evaluating the seismic performance of reinforced masonry coupled shear wall systems despite its use throughout masonry buildings. The current study presents the results obtained from testing of two coupled RM shear walls with different coupling distances. The walls were tested under reversed displacement based quasi-static cyclic loading. All parameters were kept constant except for the coupling distance (and thus stiffness and strength) to study the effect of the degree of coupling (DOC). The walls were specifically not design as a coupled wall SFRS, and thus, the coupling slabs were reinforced meeting only the minimum slab reinforcements requirements. The paper alos discusses the ultimate load capacity reached by the walls and displacement ductilities attained at different wall performance levels.

KEYWORDS: coupled walls, degree of coupling, ductility, plastic hinges, reinforced masonry, shear walls, stiffness

INTRODUCTION
Masonry shear wall building systems are a cost effective seismic force resisting systems (SFRS). From a designer's perspective, the system offers high in-plane strength and stiffness, which are beneficial in resisting large seismic forces and in providing sufficient in-plane stability. In order to account for doors, windows, pathways and service ducts, openings must be provided within a shear wall system, thus possibly creating a coupled wall system. A planar coupled shear walls may be defined as a structural system composed of a number of shear walls which are interconnected by a series of spandrel beams or concrete slabs. [1,2] During moderate and high earthquake events these systems will often respond beyond their elastic limit. The dynamic behaviour of coupled shear wall systems is quite different from typical cantilever walls. The formation of new plastic hinge regions at the interface of the beams and walls complicates the behaviour of the walls and might entail additional rotational capacity demands. As such,

designers of such system should give special attention to the rotational demand at the plastic hinges and ensure it does not exceed the rotational capacity of the component.

The current Canadian concrete code A23.3 sets two separate R_d factors for ductile coupled shear walls and partially coupled shear walls. The ductile coupled shear walls are set to a value of R_d=4.0 while the other wall type is set to R_d=3.5. On the other hand, the current masonry code, S304.1, provides no R_d factors for coupled masonry walls. The current study discusses ductility capacity obtained by reinforced masonry shear walls with different degree of coupling and compares their displacement predictions with the test results.

BACKGROUND ON COUPLED WALLS

The behaviour of coupled walls system can be divided into two categories (i) A weak wall-strong connection mechanism and (ii) a strong wall- weak connection mechanism. The second mechanism is the desired one because it prevents catastrophic soft storey failure from developing. In a properly designed coupled wall system, the collapse mechanism is defined by the formation of plastic hinges at the bottom of the walls and in the coupling slabs or beams. An important assumption is made here where all the plastic deformation is concentrated in these regions and the walls rotation results from the formation of plastic hinge zones. Since the slabs or beams are the critical element during the coupling mechanism, it is important to compute the slabs plastic rotation capacity to define the rotational ductility of the coupled wall system. As stated in Gilberto (1991), the coupling slab or beam plastic rotation is a function of the walls length l_w, the coupling distance l_b, the plastic displacement Δ_p, number of storeys n, and total height h as illustrated in Equation 1 [3]

$$\theta_{pb} = \left(1 + \frac{l_w}{l_b}\right) \times \frac{\Delta_p}{nh} \quad (1)$$

The rotational ductility demand can be then calculated from Equation 1 by dividing by the slab yield rotation θ_{yb}:

$$\mu_{\theta b} = \frac{(1 + l_w/l_b)}{nh} \times \frac{\Delta_y}{\theta_{yb}} (\mu - 1) + 1 \quad (2)$$

Where Δ_y is the top yield displacement of the wall and μ is the overall displacement ductility of the coupled wall system. When insufficient transverse reinforcement is provided, the coupled walls develops a premature shear failure in the coupling slabs or beams, thus limiting the effectiveness of the coupled wall system. This problem can be resolved when the span to depth ratio of coupling beams is small (less than 2.0) by introducing detailed diagonal reinforcement as suggested by Paulay and Binney (1974). For higher span to depth ratios of coupling beams, Shiu et al. (1978) proved the ineffectiveness of the special diagonal reinforcements. [4]

Within the scope of this study, the degree of coupling (DOC) will be defined as the percentile ratio of the overturning moment carried by the axial force (either compression or tension as a result of shear developed in the coupling element) to the overall moment. A clearer presentation of the DOC is shown in Fig. 1 below.

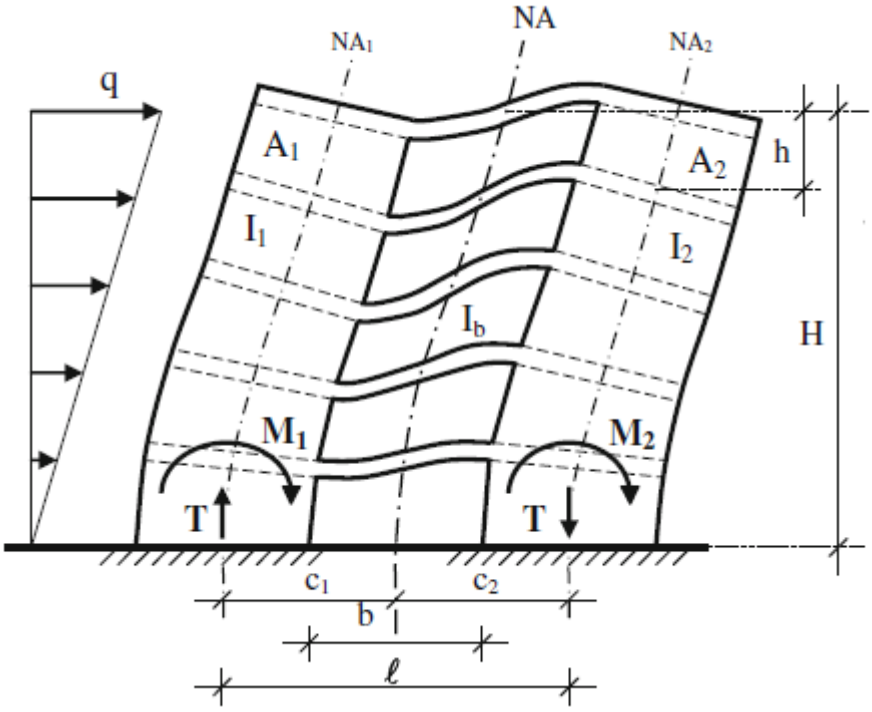

Figure 1 Coupling Action and Degree of Coupling [2]

This also indicates that the DOC depends on the relative strength between the slabs and the walls. Such definition is in compliance with the Canadian concrete code (CSA A23.3) as indicated in Equation 3 below:

$$DOC = \frac{Tl}{Tl + M_1 + M_2} \qquad (3)$$

In reinforced concrete, according to Paulay and Priestly (1992), one cannot ignore the coupling provided by slabs although is not as significant as beam coupling. When subjected to large shear forces, slabs develop moments and form yield lines and, as a result, significant shear transfer across the coupled wall system occur. The portion of the slab at a distant away from the wall planes will not be as efficient in the coupling action because transverse bending and torsional distortion reduce curvature near the edges. As such, most of the shear transfer will occur mainly around the edges of wall section where also maximum slab curvature levels develop. [5]

EXPERIMENTAL PROGRAM

Details about the constitutive materials used, its strength and the test setup are provided in another study by Siyam et al. (2010). [6] The walls were built with one third scale masonry units with average compressive strength of 25 MPa. The compressive strength of masonry (f'_m) was 19.3 MPa for the lower wall sections and 17.3 MPa for upper wall sections. The main reinforcement had yield strength (f_y) of 495 MPa. The two walls, shown in Fig. 2, were tested under quasi-static displacement based cyclic loading applied evenly to the top wall slab. The loading scheme was divided into two phases (i) a force-controlled phase where the wall has being cycled with increments of the predicted yield load and (ii) a displacement-controlled phase

where the walls has been cycled into increments of yield displacement. The loading history used in the testing is shown in Fig. 3. The loading was applied through a specially fabricated loading beam that facilitated wall rotation without adding to the flexural capacity of the walls. All of the dimension details and reinforcement information along with the coupling distance pertaining to the walls is shown in Table 1. As evident from the table, all the parameters are kept constant except for the coupling distance. The difference in the coupling distance will lead to different DOC in the two coupled wall systems.

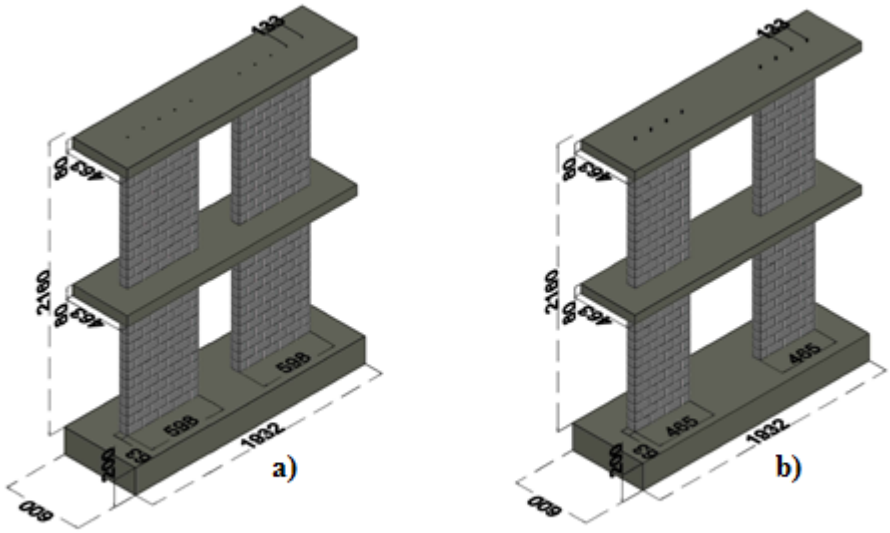

Figure 2 Coupled walls: a) Low coupling distance b) High coupling distance

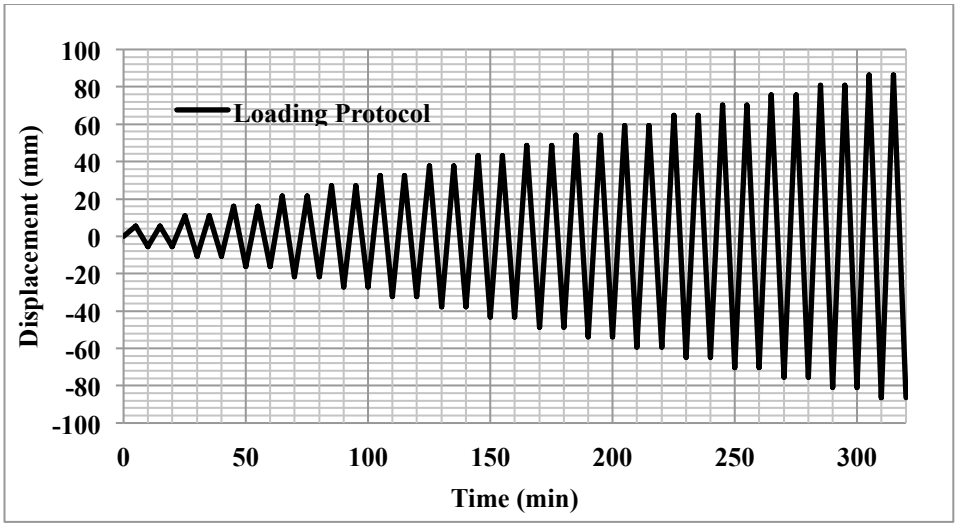

Figure 3 Loading History

Table 1 Walls details and Specifications

Wall	Height (mm)	Length (mm)	Coupling Distance	Vertical reinforcement		Horizontal reinforcement		
				φ_v (mm)	ρ_v(%)	φ_h (mm)	ρ_{h1} (%)	ρ_{h2} (%)
1	2,160	1,533	937	7.6	0.59	3.8	0.26	0.14
2	2,160	1,533	1,070	7.6	0.61	3.8	0.26	0.14

TEST RESULTS

Wall 1 represents the coupled walls with clear span coupling distance of 305 mm (915 at full-scale). The wall hysteresis relationship showed a symmetric response in the push-pull directions (Fig 4). The onset of bed joint cracking occurred at 60% of the yield load at 16.3 kN with a 3.2 mm average displacement. Slab cracks were first noticed at 80% of the yield load (21.7 kN) corresponding to 4.95 mm displacement. Continued load reversals further extended the formed bed-joint cracks, and initiated new bedjoint, head joint, shear, and slab cracks. The first head joint cracks and shear cracks occurred at yield load (33.9 kN) producing a yield displacement Δ_y of 10.3 mm. This occurred on the West wall which appeared to be slightly stronger than the East one, evident by the higher loads and lower displacements. The bedjoint cracks kept propagating until the 5th course of the second floor. During the second phase of the testing, crushing at the internal wall top corners occurred at $2\Delta_y$ (Δ_{top} = 20.6 mm) displacement cycle. The latter is attributed to the load transfer at the wall/slab interface. At 1.9% drift there was significant masonry crushing at the toes. This point marked the maximum load capacity of the wall (43.4 kN). Further displacement cycles ($5\Delta_y$ and $6\Delta_y$) induced buckling (under compression) and fracture (under tension) of wall end reinforcement bars. The test was terminated when the two end bars fractured during the push and pull cycles marking 51% ultimate load degradation (22.4 kN) at 3.3% drift.

Wall 2 represent coupled wall with a coupling distance 605 mm, almost double that of Wall 1. As such, the wall system was less stiff than Wall 1. The wall showed a slight asymmetry in terms of load-displacement relationship during the first test phase but then exhibited a symmetric response afterwards. Similar to Wall 1, initiation of bed joint cracking commenced at 60% yield load (13.2 kN) corresponding to 4.9 mm displacement. The first slab crack appeared on the bottom side of first floor at 80% F_y where the wall reached a displacement of 9.7 mm. At yield load (22.3 kN), these cracks surrounded all slab faces. Severe bed joint cracking occurred at the first floor, where most of the hinging mechanism occurred, and continued to develop up to $3\Delta_y$ (Δ_{top} = 36.9 mm) displacement cycle corresponding to 27 kN lateral load. The second storey had a number of bed joint cracks developing at $2\Delta_y$, $3\Delta_y$, and $4\Delta_y$ displacement cycles. These cycles also corresponded to high lateral loads. Few shear cracks were also noticed at $3\Delta_y$ cycle. The wall reached a maximum lateral load of 28 kN at 1.1% drift during the push cycle. Continued displacement cycles propagated vertical splitting cracks at the wall toes, which lead to masonry and grout crushing. At this stage, the wall reached a drift capacity of 2.8%. Final cycles resulted in buckling of extreme vertical reinforcements in the East and West walls as the respective bars were subjected to compression. During the second cycle of $6\Delta_y$ (Δ_{top} = 73.8 mm), the reinforcement bars fractured, which subsequently resulted in the lateral load dropping by 55% (15.6 kN) corresponding to 3.4% ultimate drift capacity.

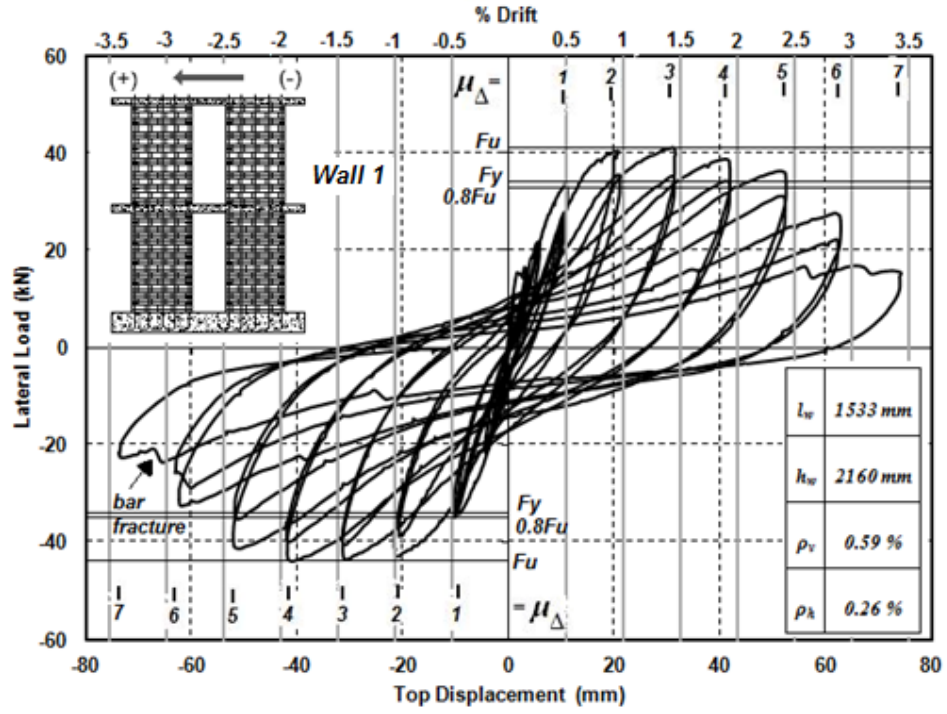

a)

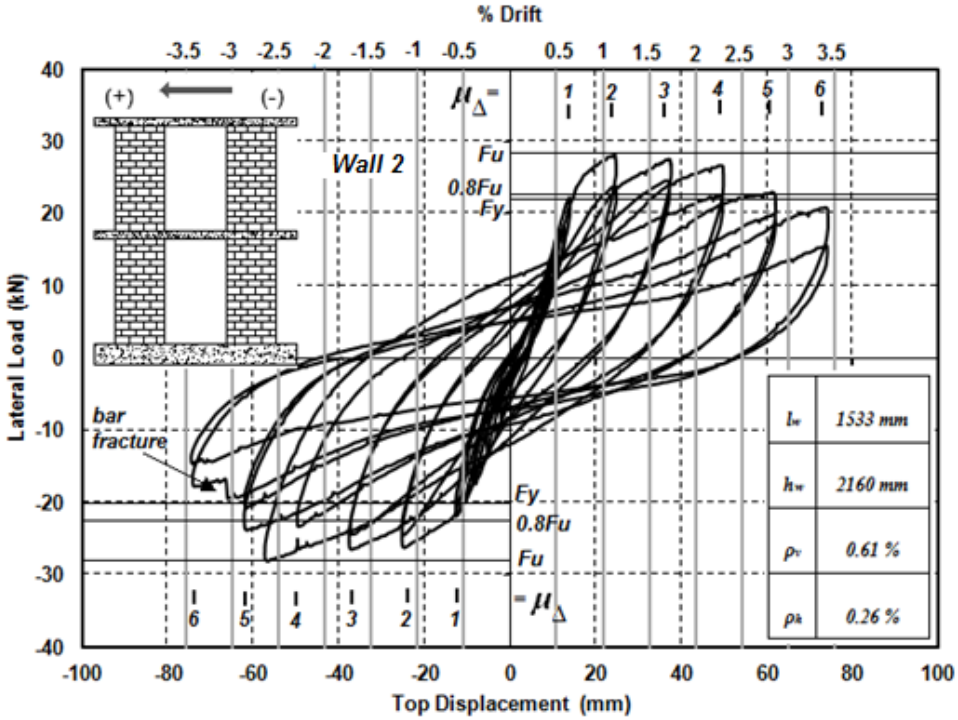

b)

Figure 4 Load-displacement relationships of the two coupled wall systems

MODELLING OF COUPLED WALLS

Coupled walls can be modelled using two vertical beam-column elements linked by coupling beam element at each floor level. A model discretization is shown in Fig. 5. The wall is modelled using frame systems where the walls are discretised as beam-column elements at the wall centre of gravity with rigid zones (links) representing half the wall length at each slab-to-wall connection. The rigid links at the wall ends were connected to beams element representing the slabs. The bases of the wall elements were fully restrained. The model is constructed using SeismoStruct software. [7] The walls and slabs were modelled using their geometrical and cross sectional material properties as inelastic displacement based elements. The experimental cyclic protocol was applied to the top wall nodes. The elements are drawn at its centroidal axis with the slab element covering only the clear span between the two walls. [8]

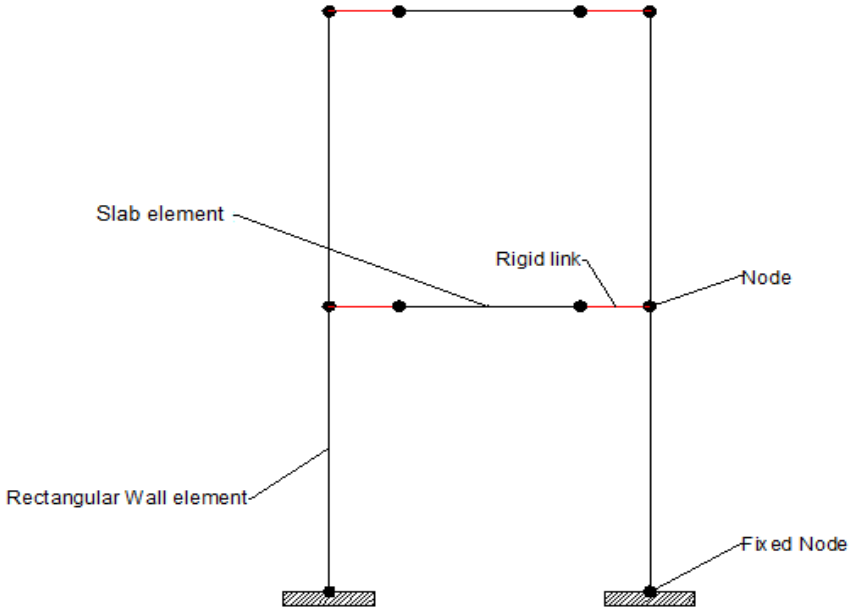

Figure 5 Model Discretization

Concrete constitutive relation is used to represent the fully grouted masonry material with its nonlinearity because of the resemblance of fully grouted reinforced masonry to reinforced concrete. The walls are modelled using SeismoStruct's concrete unconfined material with f'_m values obtained from prism tests as 19.3 MPa and 17.3 MPa representing the wall sections on the first and second storey, respectively. The reinforcement were modelled using Menegotto and Pinto model (1973) The cyclic load has been identified in the software using Fig 3 loading protocol. The hysteresis curves for Walls 1 and 2 have been superimposed on the experimental hysteresis curves presented earlier in Fig. 4 as shown in Fig. 6. The models capture the shear wall yield loads and their ultimate capacities (listed in Table 2) fairly well. F_y and F_u in table 2 denotes the yield and ultimate load respectively. However, some inaccuracies in the energy dissipation (i.e. the area within the hysteresis loops) and the strength degradation characteristics of the model can also be observed. As a result, the failure load and ultimate displacements are overestimated by the models.

Table 2 Experimental and Seismo-Struct Yield and Ultimate loads

Wall	Experimental load		Seismo-Struct Model		% Difference in F_y	% Difference in F_u
	F_y (kN)	F_u (kN)	F_y (kN)	F_u (kN)		
1	33.9	42.3	32	44.6	5.60%	-5.44%
2	21.3	27.4	22	31.3	-3.29%	-14.23%

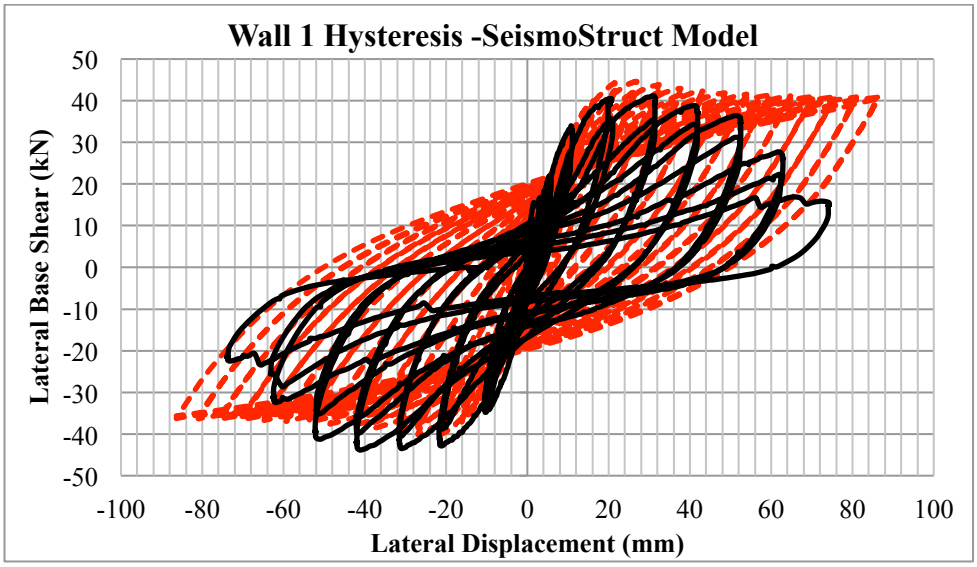

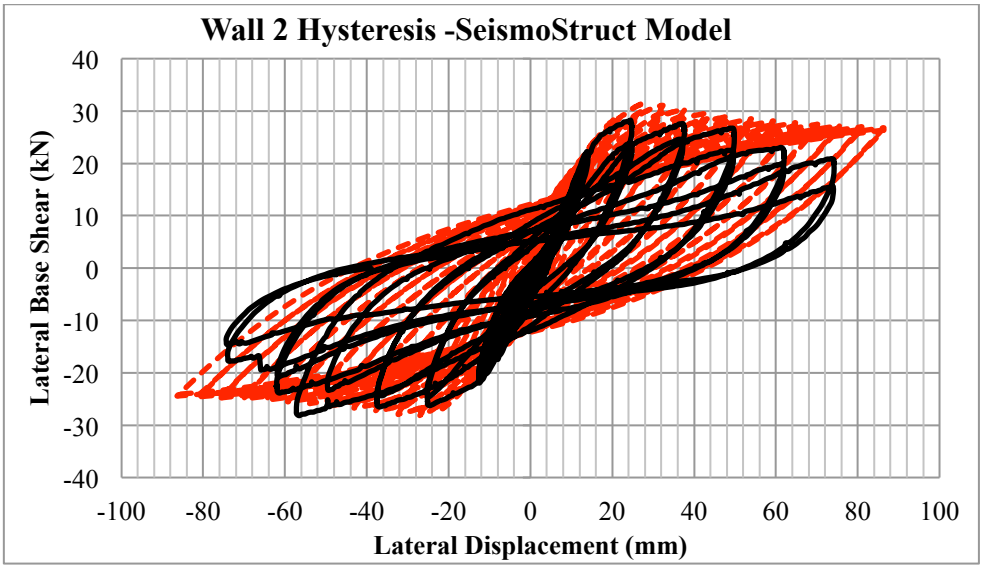

Figure 6 Model Wall Hysteresis

DISPLACEMENT CAPACITY AND DUCTILITY OF THE COUPLED WALLS

The procedure suggested by Paulay (2002) is used to predict the coupled wall performance in terms of yield, and ultimate curvature and displacements. [9] Both the slab and the wall performance parameters are predicted and compared to the ones obtained from the experimental results. Paulay suggests that nominal yield displacement and rotation of the coupled wall is achieved when the wall maximum base curvature reaches the nominal yield curvature. It is known that the maximum drift and rotations occurs at the height of the wall having zero moment (the contra-flexure height h_{cf}). The maximum nominal yield displacement and rotation of the *wall* can then be predicted using Equations (4) and (5): [10]

$$\Delta_{wy} = \frac{\phi_{wy} h_{cf}^2}{3} \qquad (4)$$

$$\theta_{wy} = \frac{\phi_{wy} h_{cf}}{2} \qquad (5)$$

Where ϕ_{wy} is the nominal yield curvature which is found to be a function of wall length l_w and longitudinal reinforcement yield strain ε_y according to Priestly et al. (2007) approximation for reinforced masonry walls:

$$\phi_y = \frac{2.1\epsilon_y}{l_w} \qquad (6)$$

After the wall curvature is obtained one can compute the yield rotation of coupling slab using Equation 7 assuming the rotation happens at the centre of the walls (see Fig. 7)

$$\theta_{CB} = \theta_w(1 + l_w/L_{CB}) \quad (7)$$

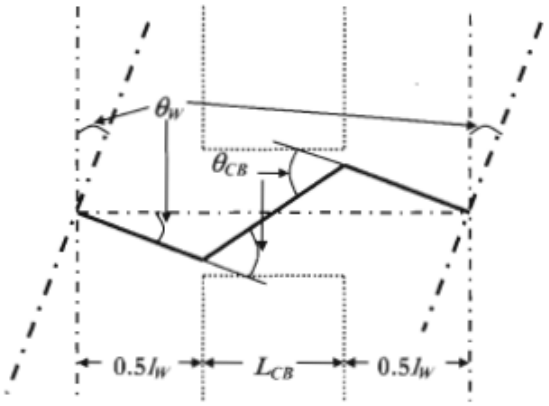

Figure 7 Coupled Wall rigid mechanism (Priestly et al. 2007) [10]

θ_{CB} and θ_w denotes the coupling beam and wall rotations respectively and l_w, L_{CB} symbolize the wall and the coupling beam lengths. Subbing Equation 5 into Equation 7, the maximum rotation of the coupling beam at the wall's nominal yield will be:

$$\theta_{CB,wy} = 0.5\phi_{wy} h_{cf}(1 + l_w/L_{CB}) \qquad (8)$$

In addition, the slab yield rotation is calculated using Equation 9:

$$\theta_{y,CB} = 0.35\epsilon_y \frac{L_{CB,eff}}{h_{CB}} \qquad (9)$$

Where $\theta_{y,CB}$, h_{CB}, ϵ_y and $L_{CB,eff}$ symbolizes the slab yield rotation, depth of the slab, strain of reinforcement and extended effective length of the coupling slab taking into account tensile strain penetration. $L_{CB,eff}$ can be expressed as follows:

$$L_{CB,eff} = L_{CB} + 2h_{CB} \qquad (10)$$

As suggested in Priestly et al. (2007), there are three cases that might govern the displacement capacity of coupled reinforced masonry shear walls, the wall base strain, the code limitation on wall drift at the contra-flexure height (h_{cf}), and the strains in the coupling elements. The case providing the least displacement will lead to the governing capacity of the coupled shear wall system. The three equations for each case are shown below:

Case I: *Wall Base Strain Case*: $\Delta = \Delta_y + (\phi_{ls} - \phi_{wy})L_p h_{cf}$ (11)

Where ϕ_{ls} symbolizes the wall material strain at a specific performance level i.e. ultimate

Case II: *Wall Drift at* h_{cf}: $\Delta = \Delta_y + (\theta_C - 0.5\phi_{wy}h_{cf})L_p h_{cf}$ (12)

Where θ_C is the code specified drift limit.

Case III: *Material strain in the coupling element*:

The rotation capacity of the coupling beam/slab θ_{ls} can be obtained from Equation 11 above and replaced by θ_C in Eq. 12, yielding the following expression. [10]

$$\Delta = \Delta_y + (\theta_{ls} - 0.5\phi_{wy}h_{cf})L_p h_{cf} \qquad (13)$$

Table 3 sums the predicted yield curvatures and displacement for the wall and the slab using the formulas above.

Table 3 Displacement based parameter predictions of Coupled Walls

Wall	Wall length (mm)	Degree of Coupling (θ_{CB})	Yield Curvature (φ_y)	Yield Displacement (mm) (Δ_{wy})	Yield Rotation (ϑ_{wy})	Maximum rotation of slab at wall yield ($\vartheta_{CB,wy}$)	Slab yield rotation $\vartheta_{y,CB}$
1	598	0.22	8.69147E-06	6.623	0.00657	0.0182	0.00538
2	465	0.38	1.11774E-05	8.518	0.00845	0.0201	0.00827

Table 4 illustrates the results of coupled wall displacements and ductility predictions using the three cases mentioned before. In addition the rotational ductility of the slab is calculated using Equation 2, proposed in Gilberto (1991), [3] for the governing case. The governing displacement capacity for the coupled walls was attributed to the strain in the coupling slab resulting in displacement limits of 24.3 mm and 26.2 mm for Walls 1 and 2, respectively. The corresponding displacement ductility levels were 3.66 and 3.07. An important assumption was made in the computation of the yield and ultimate curvatures where the length of one wall has been used to come up with the displacements.

Table 4 Coupled wall Displacements and Ductility predictions

Wall	Coupled Wall Displacement (Δ_w) (mm)			Displacement Ductility (μ_Δ)			Rotational Ductility ($\mu_{\vartheta b}$)
	Wall base Strain	Wall Drift at h_{cf}	Material Strain in the coupling slab	Wall base Strain	Wall Drift at h_{cf}	Material Strain in the coupling slab	
1	50.86	42.05	24.25	7.68	6.35	3.66	3.92
2	67.83	41.10	26.15	7.96	4.83	3.07	2.06

The predicted values obtained in Table 4 are compared with the experimental values in Table 5. Different limit states was identified in acquiring the experimental results, only two are shown in Table 4, displacement at maximum load and at 20% load degradation. The predictions corresponds well with the first limit state ductility level with percentage error of 3.1% and 5.1% for Walls 1 and 2 respectively. Nevertheless, reinforced masonry coupled walls shows capabilities of reaching displacement ductility levels up to 5 as shown in Table 4.

Table 5 Experimental Coupled wall Displacements and Ductility

Wall	Experimental Coupled Wall Displacement (Δ_w) (mm)			Displacement Ductility (μ_Δ)	
	Yield (Δ_{wy})	Maximum Load (Δ_{um})	20% Load Degradation ($\Delta_{0.8Fu}$)	Maximum Load ($\mu_{\Delta u}$)	20% Load Degradation ($\mu_{\Delta 0.8Fu}$)
1	10.20	36.20	58.80	3.55	5.76
2	12.40	36.20	63.70	2.92	5.14

CONCLUSIONS

Coupled walls system provides an excellent alternative to cantilever walls when it comes to selecting SFRS, as such systems typically exhibit higher levels of energy dissipation and displacement capacities when subjected to large lateral forces. The current study examined two coupled reinforced masonry shear walls subjected to increasing displacement cyclic loading. The only difference between the two walls is the degree of coupling (DOC), which is based on strength calculations of the coupling slabs and the walls. Numerical simulation was conducted for the coupled wall system using a discretized SeismoStruct software model. The hysteresis results showed very good predictions of yield and ultimate loads when compared to experimental results. However, the model is inaccurate in terms of representing energy dissipation and failure load of the walls. A displacement-based approach was used to predict the displacement and ductility of the walls. The method utilizes mechanics-based assumption to define three possibly

governing cases to quantify the wall ultimate displacement. The governing prediction was found to be the material strain in the coupling slabs. Finally the displacement ductility results acquired from the experiment indicated good agreement with the predictions especially with the maximum load limit state. At such limit state the ductility values reached were 3.6 and 2.9 for Walls 1 and 2 respectively. Reinforced masonry coupled walls shows great potential in terms of their seismic performance. The results are promising towards incorporating R_d value of at least 3.0 for a new ductile coupled masonry shear walls category in upcoming edition of the National Building Code of Canada (NBCC) 2010.

ACKNOWLEDGEMENTS

Financial support has been provided by the McMaster University Centre for Effective Design of Structures (CEDS) funded through the Ontario Research and Development Challenge Fund (ORDCF) as well as the Natural Sciences and Engineering Research Council (NSERC) of Canada. Provision of mason time by Ontario Masonry Contractors Association (OMCA) and Canada Masonry Design Centre (CMDC) is appreciated. The supply of the scaled blocks by the Canadian Concrete Masonry Producers Association (CCMPA) is gratefully acknowledged.

REFERENCES

1. El-Shafee M.O. (1976) “Elasto-Plastic Dynamic Analysis of Coupled Shear Walls” M.Eng Thesis, McMaster University, Hamilton, Ontario, Canada.
2. Chan H.B. (1971) “Static and Dynamic Analysis of Plane Coupled Shear Walls” M.Eng Thesis, McMaster University, Hamilton, Ontario, Canada.
3. Leiva G.H. (1991) “Seismic Resistance of Two Storey Masonry Walls with Openings” Ph.D Thesis, The University of Texas , Austic, US.
4. Hoenderkamp J.C.D. (2012) “Degree of Coupling in high rise mixed shear wall structures” *Indian Academy of Sciences* (37), pp 481-492.
5. Paulay, T., Priestly, M.J.N. “Seismic Design of Reinforced Concrete and Masonry Buildings” New York: John Wiley & Sons; 1992.
6. Siyam, M., El-Dakhakhni, W.W. and Drysdale, R.G. (2012) “Seismic Behaviour of Reduced Scale Two-Storey Reinforced Concrete Masonry Shear Walls” 15th International Brick and Block Masonry Conference, Florianopolis, Brazil.
7. SeismoSoft ltd. “SeismoStruct Manual”, Pavia, Italy, 2002-2012.
8. White W.T. (2004) “Seismic Demand in High-Rise Concrete Walls” Ph.D Thesis,University of British Columbia, Vancouver, Canada, in press.
9. Paulay T. “The displacement capacity of reinforced concrete coupled walls” Engineering Structures 24 (2002), 1165-1175
10. Priestly, M.J.N., Calvi G.M., Kowalsky M.J. “Displacement Based Seismic Design of Structures” Pavia: IUSS Press; 2007.